

Mapping the dark trajectory of the Bullet Cluster

X. J. Bi

*Key laboratory of particle astrophysics, IHEP,
Chinese Academy of Sciences, Beijing 100049, P. R. China*

H.S. Zhao

*SUPA, School of Physics and Astronomy,
University of St Andrews, KY16 9SS, Fife, UK*

(Dated: December 9, 2018)

Abstract

We model the electrons/positrons produced by dark matter annihilations in the colliding galaxy cluster system 1E0657-56 (the bullet cluster). These charged particles, confined by the Magnetic field, clearly trace the path of the bullet, which passes through the main cluster with a speed of 3000-5000 km/s. Adding the effect of dark matter substructure (subhalos) in each cluster we find the annihilation rate is enhanced greatly and the density of positrons in the trail is similar to that within the bullet cluster. This opens the door to unambiguous detection of the annihilation signal through the SZ effect, at significant separation from the thermal electrons.

PACS numbers: 98.10.+z, 98.62.Dm, 95.35.+d, 95.30.Sf

The nature of dark matter particles is one of the most outstanding puzzles in particle physics and cosmology. A massive effort has been made in the last decade to unravel the mystery, but to little avail. Numerous theoretical models have been proposed, among which the most attractive scenario involves weakly interacting massive particles (WIMPs). A viable way to identify WIMPs is to search their annihilation products, such as γ -rays, neutrinos, positrons or anti-protons. Up to now most efforts have focused on looking for the signals within the Milky Way. We know there are large quantities of dark matter residing in galaxy clusters. However, they are typically too distant to observe these annihilation signals directly. One viable way to look for the effects of dark matter annihilations in clusters is to compute the SZ effect produced by the non-thermal electrons/positrons which scatter off the background CMB photons [1], but are not weakened by the long distance.

However, the SZ effect from the thermal electrons in the cluster X-ray gas is usually much greater than the SZ effect from the non-thermal electrons produced from dark matter annihilations and leads to difficulties disentangling them. Colliding galaxy clusters provide one of the best systems in nature where we see a clear offset of baryonic material concentrations and the gravitational centres, which are generally interpreted as direct evidence of the long-speculated dark matter. For example, the bullet cluster system 1E0657-56 ([2], [3]) is such a system with clear spatial separation of the X-ray gas and the dark matter halos, which offers an ideal place to search for signals of dark matter annihilation.

For the bullet cluster, we observe, at optical wavelengths, two concentrations of galaxies with the smaller one passing through the larger one. Clearly the two systems are merging with one another. X-ray observations show a hot gas envelop joining both clusters, and an intense bow-shocked structure in between the optical centres. Looking past these clusters, we observe systematic weak distortions of the shapes of the background galaxies, with the signal being concentrated on the galaxies and not the X-ray gas, which is impossible if there is not more dark matter co-existing with the galaxies in some collisionless form.

The bow-shock observed in the gas distribution of the sub cluster, implies a supersonic motion of the shock of about 5000km/s in the X -direction perpendicular to the line of sight. The underlying dark matter might move somewhat slower, about 3000km/s in the recent simulation [4], but see [5] for a discussion. The centre of the X-ray emitting gas is about 300 kpc to the left (East) of the bullet, and 400kpc to the West of the main cluster.

A halo of synchrotron emission has been observed at radio wavelengths for this cluster

[6], which might be associated with the elongated emission of the X-ray gas. However, there is no indication for any enhancement near the DM clump locations. A SZ map of 1E0657-56 have also been obtained with ACBAR [7], which again does not show any enhancement, at the centres of the dark halos, although the resolution $\sim 4.5' \sim 100$ kpc at the cluster's redshift ($z = 0.3$). Recently Colafrancesco et al. [8] made a new calculation of the SZ effect by the nonthermal electrons from dark matter annihilation. They conclude that a detection of such effect is feasible in the future observations.

In the present work we propose a new effect in this system which can clearly show their origin from dark matter annihilation. Since the dark halo of the bullet cluster is offset from the thermal gas and moving with a huge speed within the main cluster we expect the electrons/positrons from dark matter annihilation in the bullet cluster will be confined by the magnetic field, which is frozen with the gas, and spread over a long trail. Further we take the subhalos into account when calculating the dark matter annihilation, which can greatly enhance the annihilation signal. The effect of subhalos also makes the electron density in the trail almost the same magnitude as that within the bullet cluster. Therefore we expect the SZ effect from this trail to be of the same order as from the main and bullet clusters and detectable in the future observation.

A promising WIMP candidate is the neutralino, the lightest supersymmetric particle, which is neutral and generally stable. Neutralinos can annihilate into a pair of quarks, leptons or gauge bosons, which decay to electrons/positrons and some other states finally. In the present work we assume neutralinos account for all dark matter in the universe.

The source function of electrons and positrons from DM annihilations can be written as

$$Q(E_e, \mathbf{r}) = \frac{\langle \sigma v \rangle}{2m_\chi^2} \frac{dN}{dE} \rho^2(\mathbf{r}) = f(E_e) \rho^2(\mathbf{r}), \quad (1)$$

where σ is the electron/positron generating cross-section, dN/dE is the electron/positron spectrum produced by one annihilation from a pair of neutralinos and $\rho(\mathbf{r})$ is the neutralino density distribution in space.

The factor $f(E_e)$ in the source term is calculated in the minimal supersymmetric standard model (MSSM) by performing a random scan in the SUSY parameter space using the software package DarkSUSY [9]. Under some simplification assumptions only seven most relevant SUSY parameters are kept, as done in DarkSUSY [9]. We require the models to satisfy the constraints from colliders and cosmology. In particular, the relic density

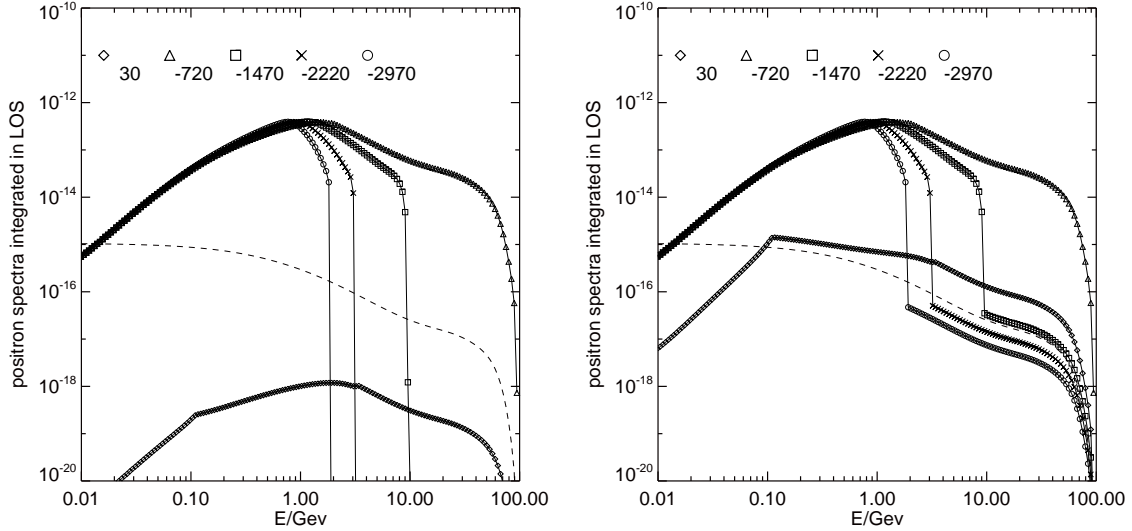


FIG. 1: Shows the line-of-sight integrated spectrum $\int_{-\infty}^{\infty} E^2 n_e(E, x, y = 0, z) dz$ for different positions on the X-axis ($x = 30, -720, -1470, -2220, -2970$ kpc). Here x, y, z are the directions of the bullet’s motion, distance from the cluster centers and along the line of sight. Here we compare the steady-state spectrum (dashed line which levels off at low energy, $x = 30$ kpc) with the moving model (left) and moving model with substructure (right). The spectrum is softer near the “tail” of the bullet.

$0 < \Omega_\chi h^2 < 0.118$ is required, which is lower than the 3σ upper bound from the cosmological observations [10]. For the small relic density we assume a nonthermal production mechanism [11]. Among the randomly produced 1000 models we choose a model which has a large branching ratio to electrons and positrons. Here we produce only 1000 models in order not to introduce too large fine tuning of the SUSY parameters.

The second factor $\rho^2(\mathbf{r})$ in Eq. (1) is determined by the dark matter distribution. We model the two clusters with NFW profiles, as shown in [4] and adopt the following structure parameters: $M_{vir} = 1.5 \cdot 10^{15} M_\odot$, $R_{vir} = 2.3$ Mpc and $c_{vir} = R_{vir}/r_s = 3$ for the larger (East) DM halo; $M_{vir} = 1.5 \cdot 10^{14} M_\odot$, $R_{vir} = 1.070$ Mpc and $c_{vir} = 7.2$ for the “bullet” (West) DM clump. This mass profile approximates the signal of weak gravitational lensing satisfactorily.

For substructures within each cluster we have the number density of substructures with

mass m_{sub} at the position r to the cluster center as [12]

$$n(m_{\text{sub}}, r) = n_0 \left(\frac{m_{\text{sub}}}{M_{\text{vir}}} \right)^{-1.9} (1 + (r/r_H)^2)^{-1} , \quad (2)$$

where M_{vir} is the virial mass of the cluster, n_0 is the normalization factor determined by requiring that about 50% of the dark matter is enclosed in the subhalos [13]. We take the minimal subhalo to be as light as $10^{-6}M_{\odot}$ as shown in the simulation by Diemand et al. [13] and the maximal subhalo about $0.01M_{\text{vir}}$. To determine the profile of each subhalo we adopt the semi-analytic model of Bullock et al. [14] to give the concentration parameter c_{vir} as a function of the subhalo virial mass. Simulation also shows [14] that subhalos in dense environment usually have larger concentration parameters than the corresponding distinct halos with same mass. Here we take a factor of 2 larger than the concentration parameter given by the Bullock model.

Taking the subhalos into account, the density squared term in Eq. (1) is replaced by

$$\rho^2(\mathbf{r}) \rightarrow \langle \rho^2(\mathbf{r}) \rangle = \rho_{\text{smooth}}^2(\mathbf{r}) + \langle \rho_{\text{sub}}^2(\mathbf{r}) \rangle , \quad (3)$$

where $\langle \rho_{\text{sub}}^2(\mathbf{r}) \rangle$ means the average density square of subhalos according to the subhalo distribution probability. Since there is no correlation between the mass and spatial distribution in Eq. (2) we get $\langle \rho_{\text{sub}}^2(\mathbf{r}) \rangle$ at the position \mathbf{r} from an integral over mass

$$\langle \rho_{\text{sub}}^2(\mathbf{r}) \rangle = \int_{m_{\text{min}}}^{m_{\text{max}}} n(m_{\text{sub}}, r) \left(\int \rho_{\text{sub}}^2 dV_{\text{sub}} \right) \cdot dm_{\text{sub}} ,$$

where ρ_{sub} refers to the density of the subhalo at \mathbf{r} and V_{sub} is its volume.

When the bullet crosses the main cluster, the dark matter density at each point is the sum of the two individual clusters and changes with time. Therefore the annihilation signal is enhanced due to the superposition of the dark matter density of the two clusters. A detailed match of CDM models with the Mach-cone in the X-ray suggests that the two CDM halos are presently moving with about 3000km/s to each other. The speed was initially 1800km/s at the contact of the two halos and was maximized to 4000km/s when the two cluster centers coincide. Overall we take an average of 3000km/s as suggested in the recent model of Springel and Farrar [4].

The electrons/positrons from dark matter annihilation will undergo the processes of diffusion and energy loss in the intracluster medium. The diffusion equation is

$$\frac{\partial}{\partial t} \frac{dn_e}{dE} = \frac{\partial}{\partial E} \left(b(E) \frac{dn_e}{dE} \right) + Q(E, t; \mathbf{r}) , \quad (4)$$

where we have dropped the spatial diffusion term since the diffusion time scale is longer than that of energy loss for electrons/positrons with $E \gtrsim 10\text{MeV}$ [1], and $b(E) = -\frac{dE}{dt}$ is the cooling function. It should be noted that the source function here is time-dependent with the motion of the bullet cluster, which is different to that in Eq. (1).

The energy loss of electrons/positrons comes mainly from the inverse Compton effect and synchrotron radiation [1]. Neglecting the Coulomb scattering and bremsstrahlung, which are not important for the energy range that we are interested in, we get [1]

$$b(E) = b_0 \left(\frac{E}{1\text{GeV}} \right)^2 = (b_{IC}^0 + b_{syn}^0 B_\mu^2) \left(\frac{E}{1\text{GeV}} \right)^2, \quad (5)$$

with a Magnetic field $B_\mu \approx 1\mu\text{G}$ inside the virial radius of the main cluster. The simple form of $b(E)$ leads to a simple analytical solution of the transport equation (4) given bellow. (The full solution of the diffusion equation with time dependent source terms is given by Baltz and Wai [15].)

The source term Q can now be expressed as

$$Q(E, t; \mathbf{r}) = \rho_X^2(t; \mathbf{r}) f(E), \quad (6)$$

with the underlying dark matter density given as

$$\rho_X(t; \mathbf{r}) = \sum_{i=1}^2 \rho_{NFW}(|\mathbf{r} - \mathbf{r}_i(t)|) + \rho_{sub}(|\mathbf{r} - \mathbf{r}_i(t)|) \quad (7)$$

$$= 0, \quad t \leq 0 \quad (8)$$

which is decomposed into a smooth term and a substructure term, and summed over both clusters $i = 1, 2$. The coordinates of the cluster centers in the past are given by

$$\mathbf{r}_i(t) = \mathbf{r}_{i,now} + \int_t^{t_{now}} \mathbf{V}_i dt', \quad (9)$$

where $\mathbf{r}_{i,now}$ are the present positions of the cluster centers, and \mathbf{V}_i are their velocities in the past. We take the simple assumption of a head-on collision with a constant speed $V = 3000\text{km/s}$ for the bullet and zero for the main cluster.

The solution at any epoch t , position \mathbf{r} and energy E is

$$n_e(E, \mathbf{r}, t) = \frac{1}{b(E)} \int_E^{m_x} dE_e Q(E_e, t_e; \mathbf{r}) \quad (10)$$

with the emitting time

$$t_e = t - \tau(E \leftarrow E_e) = t - \int_E^{E_e} \frac{dE'}{b(E')} = t + \frac{1}{b_0} \left(\frac{1}{E_e} - \frac{1}{E} \right), \quad (11)$$

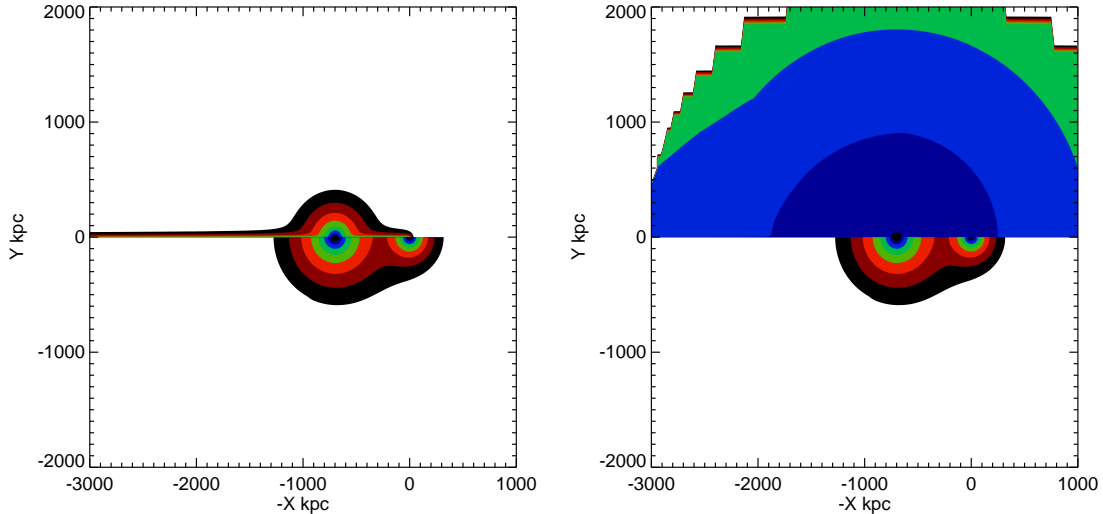


FIG. 2: shows the e^-e^+ pressure distribution $p(x, R) = \int n_e(E, x, R) E dE$ in the XR plane (no projection, $R = \sqrt{y^2 + z^2}$). Here we compare the standard double-NFW steady-state model (lower half of two panels) with our moving bullet model (upper left half with “tail”) and moving bullet with substructure model (upper right half). The bullet is the smaller cluster at $X = Y = Z = 0$, is moving further to the right with 3000km/s. Contour spacing is 0.5 dex.

where τ is the time to cool an electron from E_e to E . The initial condition is taken as $n_e = 0$ at about 10Gyrs ago.

A general practice has been to assume the electrons reach equilibrium and have a static solution of Eq. (4) with $\frac{\partial}{\partial t} n_e(E, \mathbf{r}, t) = 0$. However, we will show below that the time dependent spectrum is different from the static solution adopted in previous works [8]. This is because the time scale of energy loss for low energy electrons is longer than the source production time and has not reached its static state, as shown in [1].

In Fig. 1 we show the electrons/positrons spectra at different positions compared with the static spectrum. At high energy our spectra is the same as that of the static solution at the corresponding positions while at low energies our spectra coincides with that of the original spectrum multiplied by the time the source has existed. This means for low energy electrons the energy loss is negligible. We noticed an interesting feature of the spectra at the tail which have a break energy, above which the electrons lose energy rapidly and reached equilibrium, while below which the electrons lose energy slowly and leave the trace of the bullet passing with much higher fluxes. The effect of substructures enhances the annihilation

signal greatly at large radii. However tidal force disrupts subhalos near the cluster center [16]. Therefore the signal at $X = 30$ kpc is enhanced greatly. At other positions with high energies signals are also greatly enhanced since the static spectra at these positions are enhanced. At low energies the spectra are not determined by the local density, but by the accumulating history and dominated by the flux of the cluster center when it passes these positions. (Note we are considering the positions with $Y = 0$). Therefore substructures do not change the low energy spectra. (Certainly low energy spectra are enhanced at positions with $Y \neq 0$, see Fig. 2.)

A good indicator of the SZ effect is the non-thermal pressure

$$P(\mathbf{r}, t) = \frac{1}{3} \int_0^{E_{max}} n(E, \mathbf{r}, t) E dE \quad (12)$$

for the relativistic electrons. The trail caused by the bullet's motion shows up in projection. The inclusion of the subhalos significantly enhances the annihilation and makes the trail more obvious. In Fig. 2 we show contours of the pressure in different cases: two clusters with the static spectrum solution of Eq. (4) as adopted in [8] without motion, two clusters with motion with and without contribution from subhalos. From the figures we clearly see the trail produced by the motion of the bullet cluster. We also notice that the strength of pressure at the trail decreases further from the bullet cluster. However, considering the contribution from the subhalos reduces the attenuation.

The non-thermal relativistic positrons/electrons from annihilation distort the CMB spectra at frequencies much higher than the usual SZ-effect due to keV thermal electrons. We note that the original conclusion of Colafrancesco et al. [8] that the non-thermal SZ signals of the DM are both separable from the thermal SZ-effects and detectable with future experiments remains valid for our model: the earlier model likely underestimated the boosting factor of annihilation due to the internal substructures inside each NFW cluster halo. More importantly angular resolution is less critical because of the larger separation (about 2000 kpc, or 13 arcmin) between the positron tail from the thermal electrons; in Colafrancesco et al's case, the separation is only about 200 kpc, which is near the resolution of ground experiments like South Pole Telescope [17], Actama Cosmology Telescope [18], and balloon-borne experiments like OLIMPO [19]. The relaxed thresholds for sensitivity and angular resolution should increase the chance of annihilation-induced SZ effects being detected. The detection of a trail-like SZ signal would compound the proof of dark matter in the bullet

cluster [2].

In conclusion we consider a new effect to search the WIMP annihilation signal in the colliding bullet cluster system 1E0657-56. We find the motion of the bullet cluster will leave a clear trail of the annihilated electrons/positrons, which may lead to an observable SZ effect. In particular, taking the contribution from subhalos into account, considerably boosts the annihilation rate at large radii, meaning the pressure of the non-thermal electrons decreases slowly after the bullet has passed.

Acknowledgments

H.S.Zhao thanks PPARC and CAS, and X.J. Bi thanks Royal Society. X.J. Bi is supported by the NSF of China under the grant Nos. 10575111, 10773011 and supported in part by the Chinese Academy of Sciences under the grant No. KJCX3-SYW-N2.

-
- [1] S. Colafrancesco, S. Profumo, P. Ullio, *Astron. Astrophys.* **455**, 21 (2006).
 - [2] D. Clowe, et al. 2006, preprint astro-ph/0608407
 - [3] G.W. Angus , H.Y. Shan, H.S. Zhao, B. Famaey, *Astrophys. J.* 654, L13 (2007).
 - [4] V. Springel, G. Farrar, astro-ph/0703232.
 - [5] G.W. Angus, S.S. McGaugh, 2007, *Mon. Not. R. Astron. Soc.* in press, arXiv(0704.0381v2)
 - [6] H. Liang, et al., *Astrophys. J.* , 544, 686 (2000).
 - [7] P. Gomez, A.K. Romer, J.B. Peterson, astro-ph/0311263.
 - [8] S. Colafrancesco, P. de Bernardis, S. Masi, G. Polenta, P. Ullio, arXiv: astro-ph/0702568.
 - [9] P. Gondolo, J. Edsjo, P. Ullio, L. Bergstrom, M. Schelke, E.A. Baltz, *JCAP* 0407:008 (2004).
 - [10] D.N. Spergel, L. Verde, H.V. Peiris *et al.*, *ApJS*, 170, 377 (2007), astro-ph/0603449v2
 - [11] R. Jeannerot, X. Zhang, R. Brandenberger, *JHEP* 9912 (1999) 003; W.B. Lin, D.H. Huang, X. Zhang, R. Brandenberger, *Phys. Rev. Lett.* 86, 954 (2001).
 - [12] J. Diemand, B. Moore and J. Stadel, *Mon. Not. R. Astron. Soc.* **352** 535 (2004).
 - [13] J. Diemand, B. Moore and J. Stadel, *Nature* **433** 389 (2005).
 - [14] J.S. Bullock, T.S. Kolatt, Y. Sigad *et al.*, *Mon. Not. R. Astron. Soc.* **321** 559 (2001).
 - [15] E. A. Baltz, L. Wai, *Phys.Rev. D* **70**, 023512 (2004).

- [16] Q. Yuan, X.-J. Bi, JCAP **0705**, 001 (2007).
- [17] J. Ruhl, et al., Proc. SPIE, 5498, p. 11 (2004).
- [18] A. Kosowsky, New Astron. Rev., 47, 939 (2003).
- [19] S. Masi, M. Calvo, L. Conversi, et al., 2005, in Proc. of the Intern. School of Physics E. Fermi, Course CLIX, F.Melchiorri & Y.Rephaeli Eds., SIF, IOS press, p.359.